



# HHS Public Access

Author manuscript

*Chem Biol Drug Des.* Author manuscript; available in PMC 2015 July 09.

Published in final edited form as:

*Chem Biol Drug Des.* 2014 August ; 84(2): 158–168. doi:10.1111/cbdd.12315.

## ***In silico* characterization of an atypical MAPK phosphatase of *Plasmodium falciparum* as a suitable target for drug discovery**

**Christopher O. Campbell<sup>1</sup>, Daniel N. Santiago<sup>2</sup>, Wayne C. Guida<sup>2</sup>, Roman Manetsch<sup>2</sup>, and John H. Adams<sup>1,\*</sup>**

<sup>1</sup>Department of Global Health, University of South Florida, Tampa Florida 33612

<sup>2</sup>Department of Chemistry, University of South Florida, Tampa Florida 33612

### **Abstract**

*Plasmodium falciparum*, the causative agent of malaria, contributes to significant morbidity and mortality worldwide. Forward genetic analysis of the blood-stage asexual cycle identified the putative phosphatase from PF3D7\_1305500 as an important element of intraerythrocytic development expressed throughout the life cycle. Our preliminary evaluation identified it as an atypical MAPK phosphatase. Additional bioinformatics analysis delineated a conserved signature motif and three residues with potential importance to functional activity of the atypical dual-specificity phosphatase (DUSP) domain. A homology model of the DUSP domain was developed for use in high-throughput *in silico* screening of the available library of antimalarial compounds from ChEMBL-NTD. Seven compounds from this set with predicted affinity to the active site were tested against *in vitro* cultures and three had reduced activity against a PF3D7\_1305500 parasite, suggesting PF3D7\_1305500 is a potential target of the selected compounds. Identification of these compounds provides a novel starting point for a structure-based drug discovery strategy that moves us closer towards the discovery of new classes of clinical antimalarial drugs. These data suggest that MAPK phosphatases represent a potentially new class of *P. falciparum* drug target.

### **Introduction**

Malaria is a terrible affliction of people in tropical and subtropical regions worldwide, putting the health of approximately 40% of the global population at risk with pregnant women and children most vulnerable (1). Currently, artemisinin combination therapies (ACTs) are the recommended first line therapy endorsed by the World Health Organization (WHO) (2–4), which have been highly successful in treating cases of uncomplicated malaria for several years. However, recent emergence of artemisinin treatment failures in Southeast Asia has intensified efforts for new chemotherapeutic agents with alternate modes of action to decrease the further development of multi-drug resistance (4–7).

\*Corresponding author: Global Health Infectious Disease Research, 3720 Spectrum Blvd, Suite 304, Tampa, FL 33612, Tel +1 813 974 9916; Fax +1 813 974 0992; jadams3@health.usf.edu.

#### **Conflicts of Interest**

All authors confirm we have no financial or commercial conflicts of interest associated with this study.

The authors confirm we have no conflicts of interest associated with this study.

In an effort to discover new antimalarial drug targets in *P. falciparum* we are utilizing a random transposon-mediated insertional mutagenesis strategy to identify metabolic processes and pathways that are important for asexual blood-stage growth (8, 9). A forward genetic screen in the laboratory-adapted clone of *P. falciparum* NF54 discovered that a disruption of the gene PF3D7\_1305500 severely attenuated blood-stage *P. falciparum* growth (10). The primary phenotype of this mutant was due to a defect in cell cycle checkpoint with a significantly delayed progression out of pre-S phase (the trophozoite to schizont transition). The disruption was created by a single insertion of the transposon (*piggyBac*) into the ORF of PF3D7\_1305500, creating a null mutant; normal growth could be completely restored by complementation with the intact gene (10). Bioinformatic analysis determined the PF3D7\_1305500 protein product identified as homologous to the PTP superfamily and its structural characteristics similar to the Mitogen-Activated Protein Kinase (MAPK) phosphatase (MKP) subgroup. A key feature of this type of phosphatase is the tandem arrangement of a non-catalytic rhodanese domain followed by a dual-specificity phosphatase domain (11) and the gene is conserved in all *Plasmodium* species with a sequenced genome. MKPs in other eukaryotes can have similar functions and often are critical for intracellular signaling in response to numerous types of external stimuli (12–14).

The most detailed functional knowledge of signaling pathways in malaria research has revealed MAPK signaling cascades are critical components of sexual stage proliferation (11, 15–23). The MKP-type phosphatase is a likely regulator of these pathways. Interaction of the MKP with its phosphoprotein substrate depends on three conserved residues in the consensus DUSP domain binding pocket (11, 17, 24, 25). Analysis of the PF3D7\_1305500 DUSP domain revealed that only two of the three conserved residues typically present in a DUSP signature motif are present. Instead the third residue, which is typically an arginine, aligns with an isoleucine that is conserved in each of the *Plasmodium* orthologs. Absence of this specific residue may reduce but may not totally abrogate phosphatase activity; therefore, PF3D7\_1305500 is expected to have little or no phosphatase activity and possibly functioning as a pseudophosphatase (26–28). Conservation of the I to R substitution in all *Plasmodium* species is a unique characteristic indicative of an atypical MKP with an altered function within the malaria parasite lineage and requiring further study. This distinct active site and its potential involvement in regulating the MAPK pathway make this atypical MKP a promising candidate for antimalarial drug discovery. We have initiated identification of potential MKP inhibitory compounds through use of computational high-throughput screening (HTS) that allowed large sets of compounds to be investigated for possible biological activity (29). Using this method, suitable lead candidates can be identified from large drug-like data sets improving productivity and lowering costs to a level more favorable than *in vitro* screening methods, enhancing structure-based drug design (30, 31).

## Materials and Methods

### Identification of Conserved Domains and Evolutionary Lineage

The deduced amino acid sequence of PF3D7\_1305500 (MKP) was retrieved from a public database (32) and physicochemical parameters were determined using ProtParam (33). Conserved domains were identified using the Conserved Domains Database (CDD) (34),

Conserved Domain Architecture Retrieval Tool (CDART) (35), InterProScan (36, 37), Prosite (38, 39), Superfamily (40), and the Simple Modular Architecture Research Tool (SMART) (41, 42). The full deduced amino acid sequence and individual conserved domains were used with BLAST (BLASTP) to identify orthologs in NCBI protein. A multiple sequence alignment was constructed from the retrieved sequences with the lowest E-values to identify conserved regions. The phylogenetic tree was inferred using the Neighbor-joining method computing the evolutionary distance using the Poisson correlation with the Molecular Evolutionary Genetics Analysis software (MEGA5) (43–45).

### **Evaluation of Secondary Structure and Post-translational Modifications**

The secondary structure of the PF3D7\_1305500 product was evaluated using JPRED (46) and PSIPRED (47, 48). Phosphorylation sites were assessed using NetPhos 2.0 (49), which identifies serine, threonine and tyrosine phosphorylation sites, and NetPhosK 1.0 (50) to identify kinase binding sites. Prediction of a signal peptide and cleavage site was searched using Signal IP 3.0 (51). Mitochondrial and plastid targeting sequences were searched using the prediction servers Predotar (1) and PATS (52–54). N-terminal myristoylation was investigated using the Myristoylator from ExPASy (55).

### **Molecular Modeling and Structure Validation**

The three-dimensional structure of PF3D7\_1305500 has not been resolved so a homology model was built using the automated protein structure homology modeling server Swiss-Model. Suitable templates for modeling were identified using PSI-BLAST in the Swiss-Model repository (56–59). The crystal structure of MKP3 (NCBI Accession No. 1MKP\_A) was the most suitable of the available templates with greatest sequence coverage and similarity (60). The remaining residues of PF3D7\_1305500 not showing any significant similarity were not included for homology modeling. The model was assessed using the atomic empirical mean force potential with Atomic Non-Local Environment Assessment (ANOLEA), empirical force field with Gröningen Molecular Simulation program (GROMOS), and QMEAN6 (57, 61). The stereochemistry was assessed with a minimum resolution of 2.5 Å using PROCHECK (62). The final structure was also compared to the predicted secondary structure represented using DSSP and PROMOTIF (63). ERRAT plots were generated to check structure quality of the template and homology structure using a nine residue sliding window (64). This process was repeated in an iterative fashion until all the residues in the plot were not below 95% as done previously (65). The quality of the final structure was also verified using Verify 3D, Procheck and Ramachandran plots (62, 66, 67).

### **Identification of the Binding Pocket**

The binding pocket was identified using Pocket Finder and Q-site finder that uses the Ligsite algorithm (68–70). The output of the predicted binding pocket was also compared to the Computed Atlas of Surface Topography of proteins (CASTp), which uses the alpha shape theory pocket algorithm (71, 72). The identified pocket was also validated through comparison to the structural alignment of the resolved homology model and template (MKP3).

## Selection of the Compound Dataset and High-throughput *in silico* Docking

All docking and scoring calculations were performed using the 2012 Schrödinger Suite. The compound library was retrieved from ChEMBL-NTD (<ftp://ftp.ebi.ac.uk/pub/databases/chembl/ChEMBLNTD/>) and prepared using LigPrep (LigPrep v2.5, Schrödinger LLC). The homology model, made from sequence PF3D7\_1305500, was minimized using the OPLS2005 (73) force-field algorithm and the grid files were generated in GLIDE (Glide v5.8, Schrödinger LLC) (74, 75). The modeled structure was used to identify small molecular inhibitors with affinity to the predicted active site through *in silico* docking experiments using extra precision (XP) mode (75) on a Dell Precision 490 workstation with an Intel Xeon dual quad-core processors. From the results obtained, the molecule structures with the highest predicted affinity; lowest docking scores within GLIDE's error of 2 kcal/mol to the active site were selected. From this subset, the commercially available compounds were identified.

### *In vitro* parasite culture conditions

*P. falciparum* NF54 and C9 were cultured according to standard methods at 37°C (5% O<sub>2</sub> and 5% CO<sub>2</sub>, nitrogen balanced) in 5% hematocrit (O+ blood) and RPMI 1640 medium with 0.5% Albumax II, 0.25% sodium bicarbonate and 0.01 mg/ml gentamicin (76).

### *In vitro* Drug Susceptibility Assay Using SYBR Green I

Synchronized cultures were seeded into 96-well plates at 0.5% parasitemia and cultured for 96 hours under the previously stated conditions. Plates were then frozen overnight at -80°C. Plates were thawed for 15 minutes then mixed by pipetting. Eighty microliters of each well were transferred to a new 96-well plate followed by 100 µL of SYBR Green I (Sigma Aldrich) in lysis buffer (0.2 µL of SYBR Green I/mL 2X lysis buffer). Plates were covered and incubated in the dark for 1 hour at room temperature. Fluorescence intensity was measured with a SpectraMax M2<sup>e</sup> microplate fluorescence reader (Molecular Devices) with excitation and emission wavelengths of 485 nm and 525 nm respectively. The sample values were expressed in relative fluorescence units (RFU). EC<sub>50</sub> values were obtained by normalizing the values using control wells of samples cultured without drug and plotted using a one-phase exponential dose response curve using GraphPad Prism 6 (GraphPad Software Inc.).

## Results

### Evaluation of the Physical Properties of PF3D7\_1305500

Initial evaluation of PF3D7\_1305500 included an investigation of potential binding sites, phosphorylation sites, and post-translational modifications. These methods provided additional insight into potential interactions and functions of this putative phosphatase through the use of publicly available bioinformatics tools. This analysis found that there were not any significant phosphorylation sites or post-translational modifications. PF3D7\_1305500 also did not show presence of a signal peptide. The predicted secondary structure was used to validate the homology model and supported the final structure.

## Active Site Prediction

The predicted binding pocket for the PF3D7\_1305500 protein product was identified and validated using Qsite-Finder, Pocket Finder and CASTp. A total of 10 binding pockets were found and compared to the active site of the template protein. The analysis revealed that the identified pocket in the region of the signature motif was highly conserved with the template active site as predicted through the multiple sequence alignment (Figure 1). Phylogenetic analysis showed the overall evolutionary distance between the *Plasmodium* sequences and the template (Figure 2). The residues within the binding pocket include the signature motif residues of previously characterized active phosphatases. For example, the residues C383, D345 and I398 of PF3D7\_1305500 align with the conserved C293, D262 and R299 of MKP3. This comparison also suggests functional conservation can be inferred between this template and a homology model.

## Molecular Structure of PF3D7\_1305500

A crystallographic structure of PF3D7\_1305500 has not yet been resolved by experimental methods and neither is there a homologous protozoa protein that could be used for a template. The closest template available in the Swiss Model repository for homology modeling was the human phosphatase MKP3 with 21% similarity (Figure 3). The overall quality of the model predicted by ERRAT was 69.375 compared to 88.235 of the template, which was favorable considering the numerous INDELS in the primary sequence (Figure 4). Analysis and validation of the structure using the WHAT-IF web interface revealed that the structure was in agreement with standard structural conditions. Analysis of the Ramachandran plot gave a Z-score of  $-1.124$  that was within the expected ranges for well-refined structures with 89.2% of the amino acid residues in favored regions (Figure 5). All bonds were in agreement with standard bond lengths with a RMS Z-score of 0.669 and RMS deviation of 0.015. Additionally, the RMSD score from DaliLite of Ca trace between 141 aligned residues of MKP3 and the homology model of the PF3D7\_1305500 DUSP was 0.5 Å with a Z-score of 26.7 and 21% sequence identity. Conservation of the predicted site in the homology model and the validated site in the template suggests that the selected pocket was the most favorable for HTS. The combined results from these various analyses suggest that the homology model of PF3D7\_1305500 DUSP is reasonable and reliable.

## Ligand Selection and Drug Susceptibility Assay

The European Bioinformatics Institute (ChEMBL-NTD) has published open access phenotypic screening datasets that focus on neglected tropical diseases. Inhibitory compounds were previously screened against *P. falciparum* 3D7 and have a minimum inhibitory potential of 80% validated using LDH activity assays as an index of growth (GSK TCAMS Dataset) or erythrocyte-based proliferation assays (Novartis-GNF Malaria Box Dataset) (29, 77). The bioactive drug-like small molecules in the database adhere to the Lipinski rule-of-five and some provide abstracted bioactivities (78). Therefore, this collection of validated bioactive compounds represents the best, most diverse sets of compounds currently available for anti-malarial drug discovery research.

From the ChEMBL-NTD datasets, compounds were docked and ranked according to the GLIDE score. The 5% of the highest-ranking compounds were evaluated and selected on the

basis of their quality of interaction represented by the GLIDE calculation. Poses of each compound were resolved to show the theoretical interaction of each molecule with the active site residues (Figure 6). Of the most promising compounds, seven were readily available by commercial sources (390097; 7,8-Dihydroxy-2H-chromen-2-one: 524725; 1-(4-Chlorophenyl)-5-oxo-3-pyrrolidinecarboxylic acid: 533073; 2-((N-[(4-Fluorophenyl)(2-thienyl)methyl]glycyl)amino)-3-thiophenecarboxamide: 533730; 2-([N-(Diphenylmethyl)glycyl]amino)-3-thiophenecarboxamide: 525841; 3-[(E)-(1H-Benzimidazol-2-ylhydrazono)methyl]-2-chloro-7-methoxyquinoline: 579624; 2-[(2E)-2-(1,3-Benzodioxol-5-ylmethylene)hydrazino]-1H-benzimidazole: 585222; 2-[(2E)-2-(3,4-Dimethoxybenzylidene)hydrazino]-1H-benzimidazole) (Table 1) and therefore selected for the validation.

The bioactivity of the selected compounds was contrasted between the wild-type parasite strain (NF54) and an attenuated line unable to express PF3D7\_1305500 (C9) (Figure 7). These *in vitro* assays revealed that C9 had reduced susceptibility to 533073, 533730 and 579624 when compared with NF54 (Table 2). The mechanisms of action for each of these antimalarials is not known; however, considering the absence of the proposed target in the C9 parasite line it would be expected that there would be an altered response in these parasites when compared to the wild-type. Understanding the difference in susceptibility allows us to develop further studies to delineate the mechanisms of action for each of the selected molecular inhibitors.

## Discussion

Phosphorylation cascades are important regulatory process that exert their influence on cellular development through signal transduction and as a result have been investigated extensively to elucidate targets of chemotherapeutic intervention (12, 25, 79–82). These pathways are not yet fully characterized in *Plasmodium* and consequently there have not been any classes of drugs developed to target phosphorylation-dependent signal transduction cascades. Based on our preliminary understanding of PF3D7\_1305500, pathways utilizing this atypical phosphatase are involved in important cell cycle regulatory processes during intraerythrocytic asexual development. Through homology modeling of the atypical MKP DUSP domain and *in silico* high-throughput screening of its binding pocket, we investigated the possibility of PF3D7\_1305500 as a drug target. Previously, these methods were successful in identifying potential inhibitory compounds using other components of the developmental cycle (83).

In *P. falciparum*, PF3D7\_1305500 is a unique atypical phosphatase without any other identifiable paralogs in the genome. It is conserved among *Plasmodium* species as a single copy ortholog present in *P. berghei* (PBANKA\_140400), *P. c. chabaudi* (PCHAS\_140590), *P. knowlesi* (PKH\_140400), *P. vivax* (PVX\_12110), *P. cynomolgi* (PCYB\_141500), and *P. y. yoelii* (PYYM\_1407600). Conservation among the *Plasmodium* parasites, especially *P. falciparum* and *P. vivax* is favorable, since the ability to target both of these parasites with the same drug would present a clear advantage (84, 85). The conserved binding pocket in the DUSP domain homology model maintained the necessary features for activity and demonstrated an ability to accommodate an inhibitory substrate. Considering these structural



characteristics, it is likely that PF3D7\_1305500 interacts with the MAPK signaling pathway that is indispensable to *P. falciparum* development similar to its critical function in other eukaryote organisms (11, 17, 86–91). In addition, low homology with the closest mammalian orthologs is often an indicator of favorable drug targets. Since unique and conserved genes are typically under negative selection making their products essential, low homology limits adverse off-target effects in the mammalian host (83, 92).

The ChEMBL-NTD contains thousands of compounds with validated antimalarial activity profiles (29, 93, 94). In light of their inhibitory actions, the targets and mechanisms of action for most of them in *P. falciparum* are yet to be determined. Hypothetical malarial modes of action were developed for a few compounds to help facilitate their application against *Plasmodium* through historical GSK data regarding biochemical activity with human and microbial targets (29). In the previous studies, possible targets were inferred, but none of the hypothetical targets were associated with the compounds identified through the *in silico* screen in this current study.

To investigate the potential targeting of this *P. falciparum* atypical MKP by the selected inhibitory compounds, the susceptibility of NF54 wild-type parasite line was compared to the mutant *P. falciparum* clone C9, which is a genetically attenuated parasite line not expressing PF3D7\_1305500. *In vitro* growth inhibition assays revealed that compounds 524725, 533073 and 533730 have lower efficacy against mutant parasites compared to the wild-type NF54. Although further definitive studies are required this finding indicated that the MKP DUSP is a target of these compounds, enabling us to postulate it as a therapeutic target. Investigation of potential off-target activity was not feasible in this study.

## Conclusions and Future Directions

One of the main challenges to post genomic biology is translating a pathogen's genome to new drug targets to take advantage of combinatorial methods. In this study we demonstrated the ability to utilize *in silico* HTS to identify from a chemical database suitable lead candidates for novel target validated in a forward genetic screen. Greater utilization of this approach offers a great opportunity to assist drug discovery efforts and accelerating structure-based design. In practice, experimentally determined structures are preferred for *in silico* studies; however, the number of pharmaceutical targets of interest has far outpaced the ability to experimentally develop protein structures (30). As a result, homology modeling has become the popular method of investigation for the growing number of interesting pharmaceutical targets. Comparisons of docking results from both homology models and experimentally validated structures have produced comparable results (95, 96). Exploitation of multiple strategies is necessary in order to advance the base of knowledge in this field.

Our findings show a proof-of concept using *in silico* screening of available compound libraries with a *Plasmodium* protein to identify inhibitors and potentially elucidate mechanisms of action. The approach used employs both experimental and computational methods to identify drug compounds, which would be vital to the search for new antimalarial drugs. This method expedites the screening of large sets of compounds, allowing the identification of more manageable compounds sets in a reduced timeframe.

## Acknowledgments

This study was supported by funds from US National Institutes of Health (R01AI033656, R01AI094973, F31AI083053) and USF BITT Seed grant. The authors thank Robert Deschenes, Dennis Kyle, and Andreas Seyfang for their input on these studies.

## References

1. Small, I. Predotar v. 1.03 A prediction service for identifying putative N-terminal targeting sequences. *Genoplante*; 2003. Predotar v. 1.03 A prediction service for identifying putative N-terminal targeting sequences.
2. Dondorp AM, Nosten F, Yi P, Das D, Phyo AP, Tarning J, et al. Artemisinin resistance in *Plasmodium falciparum* malaria. *N Engl J Med*. 2009; 361:455–67. [PubMed: 19641202]
3. Maude RJ, Pontavornpinyo W, Saralamba S, Aguas R, Yeung S, Dondorp AM, et al. The last man standing is the most resistant: eliminating artemisinin-resistant malaria in Cambodia. *Malar J*. 2009; 8:31. [PubMed: 19228438]
4. Dondorp AM, Yeung S, White L, Nguon C, Day NP, Socheat D, et al. Artemisinin resistance: current status and scenarios for containment. *Nat Rev Microbiol*. 2010; 8:272–80. [PubMed: 20208550]
5. WHO. World Malaria Report 2011. World Health Organization; 2011. World Malaria Report 2011.
6. Wells TN, Alonso PL, Gutteridge WE. New medicines to improve control and contribute to the eradication of malaria. *Nat Rev Drug Discov*. 2009; 8:879–91. [PubMed: 19834482]
7. Takala-Harrison S, Clark TG, Jacob CG, Cummings MP, Miotto O, Dondorp AM, et al. Genetic loci associated with delayed clearance of *Plasmodium falciparum* following artemisinin treatment in Southeast Asia. *Proceedings of the National Academy of Sciences of the United States of America*. 2013; 110:240–5. [PubMed: 23248304]
8. Balu B, Chauhan C, Maher SP, Shoue DA, Kissinger JC, Fraser MJ Jr, et al. piggyBac is an effective tool for functional analysis of the *Plasmodium falciparum* genome. *BMC Microbiol*. 2009; 9:83. [PubMed: 19422698]
9. Balu B, Singh N, Maher SP, Adams JH. A genetic screen for attenuated growth identifies genes crucial for intraerythrocytic development of *Plasmodium falciparum*. *PLoS One*. 2010; 5:e13282. [PubMed: 20949012]
10. Balu B, Campbell C, Sedillo J, Maher S, Singh N, Thomas P, et al. Atypical mitogen-activated protein kinase phosphatase implicated in regulating transition from pre-S-Phase asexual intraerythrocytic development of *Plasmodium falciparum*. *Eukaryotic cell*. 2013; 12:1171–8. [PubMed: 23813392]
11. Farooq A, Zhou M-M. Structure and regulation of MAPK phosphatases. *Cellular signalling*. 2004; 16:769–79. [PubMed: 15115656]
12. Barr AJ, Knapp S. MAPK-specific tyrosine phosphatases: new targets for drug discovery? *Trends in pharmacological sciences*. 2006; 27:525–30. [PubMed: 16919785]
13. Cohen PT, Philp A, Vazquez-Martin C. Protein phosphatase 4--from obscurity to vital functions. *FEBS Lett*. 2005; 579:3278–86. [PubMed: 15913612]
14. Toth K, Djeha H, Ying B, Tollefson AE, Kuppaswamy M, Doronin K, et al. An oncolytic adenovirus vector combining enhanced cell-to-cell spreading, mediated by the ADP cytolytic protein, with selective replication in cancer cells with deregulated wnt signaling. *Cancer Res*. 2004; 64:3638–44. [PubMed: 15150123]
15. Camps M, Nichols a, Arkinstall S. Dual specificity phosphatases: a gene family for control of MAP kinase function. *The FASEB journal: official publication of the Federation of American Societies for Experimental Biology*. 2000; 14:6–16. [PubMed: 10627275]
16. Keyse SM. Protein phosphatases and the regulation of mitogen-activated protein kinase signalling. *Current opinion in cell biology*. 2000; 12:186–92. [PubMed: 10712927]
17. Farooq, a; Chaturvedi, G.; Mujtaba, S.; Plotnikova, O.; Zeng, L.; Dhalluin, C., et al. Solution structure of ERK2 binding domain of MAPK phosphatase MKP-3: structural insights into MKP-3 activation by ERK2. *Molecular cell*. 2001; 7:387–99. [PubMed: 11239467]



18. Noordman YE, Jansen PAM, Hendriks W. Tyrosine-specific MAPK Phosphatases and the control of ERK Signalling in PC12 Cells. *Journal of Molecular Signaling*. 2006; 1:4. [PubMed: 17224080]
19. Kim Y, Gentry MS, Harris TE, Wiley SE, Lawrence JC, Dixon JE. A conserved phosphatase cascade that regulates nuclear membrane biogenesis. *Proceedings of the National Academy of Sciences of the United States of America*. 2007; 104:6596–601. [PubMed: 17420445]
20. Kondoh K, Nishida E. Regulation of MAP kinases by MAP kinase phosphatases. *Biochimica et biophysica acta*. 2007; 1773:1227–37. [PubMed: 17208316]
21. Rudolph J. Cdc25 phosphatases: structure, specificity, and mechanism. *Biochemistry*. 2007; 46:3595–604. [PubMed: 17328562]
22. Andreeva AV, Kutuzov MA. Protozoan protein tyrosine phosphatases. *Int J Parasitol*. 2008; 38:1279–95. [PubMed: 18547579]
23. Szöör B, Ruberto I, Burchmore R, Matthews KR. A novel phosphatase cascade regulates differentiation in *Trypanosoma brucei* via a glycosomal signaling pathway. *Genes & development*. 2010; 24:1306–16. [PubMed: 20551176]
24. Barford D, Das aK, Egloff MP. The structure and mechanism of protein phosphatases: insights into catalysis and regulation. *Annual review of biophysics and biomolecular structure*. 1998; 27:133–64.
25. Boutros T, Chevet E, Metrakos P. Mitogen-activated protein (MAP) kinase/MAP kinase phosphatase regulation: roles in cell growth, death, and cancer. *Pharmacol Rev*. 2008; 60:261–310. [PubMed: 18922965]
26. Denu JM, Dixon JE. Protein tyrosine phosphatases: mechanisms of catalysis and regulation. *Current opinion in chemical biology*. 1998; 2:633–41. [PubMed: 9818190]
27. Hinton SD, Myers MP, Roggero VR, Allison LA, Tonks NK. The pseudophosphatase MK-STYX interacts with G3BP and decreases stress granule formation. *Biochem J*. 2010; 427:349–57. [PubMed: 20180778]
28. Wishart MJ, Dixon JE. Gathering STYX: phosphatase-like form predicts functions for unique protein-interaction domains. *Trends in biochemical sciences*. 1998; 23:301–6. [PubMed: 9757831]
29. Gamo FJ, Sanz LM, Vidal J, de Cozar C, Alvarez E, Lavandera JL, et al. Thousands of chemical starting points for antimalarial lead identification. *Nature*. 2010; 465:305–10. [PubMed: 20485427]
30. Kitchen DB, Decornez H, Furr JR, Bajorath J. Docking and scoring in virtual screening for drug discovery: methods and applications. *Nat Rev Drug Discov*. 2004; 3:935–49. [PubMed: 15520816]
31. McInnes C. Virtual screening strategies in drug discovery. *Curr Opin Chem Biol*. 2007; 11:494–502. [PubMed: 17936059]
32. Aurrecochea C, Brestelli J, Brunk BP, Dommer J, Fischer S, Gajria B, et al. Plasmo DB: a functional genomic database for malaria parasites. *Nucleic Acids Res*. 2009; 37:D539–43. [PubMed: 18957442]
33. Gasteiger, E.; Hoogland, C.; Gattiker, A.; Duvaud, S.; Wilkins, MR.; Appel, RD., et al. Protein Identification and Analysis Tool on the ExPASy Server. Humana Press; 2005. Protein Identification and Analysis Tool on the ExPASy Server.
34. Marchler-Bauer A, Lu S, Anderson JB, Chitsaz F, Derbyshire MK, DeWeese-Scott C, et al. CDD: a Conserved Domain Database for the functional annotation of proteins. *Nucleic Acids Res*. 2011; 39:D225–9. [PubMed: 21109532]
35. Geer LY, Domrachev M, Lipman DJ, Bryant SH. CDART: protein homology by domain architecture. *Genome Res*. 2002; 12:1619–23. [PubMed: 12368255]
36. Hunter S, Apweiler R, Attwood TK, Bairoch A, Bateman A, Binns D, et al. InterPro: the integrative protein signature database. *Nucleic Acids Res*. 2009; 37:D211–5. [PubMed: 18940856]
37. Quevillon E, Silventoinen V, Pillai S, Harte N, Mulder N, Apweiler R, et al. InterProScan: protein domains identifier. *Nucleic Acids Res*. 2005; 33:W116–20. [PubMed: 15980438]
38. Sigrist CJ, Cerutti L, de Castro E, Langendijk-Genevaux PS, Bulliard V, Bairoch A, et al. PROSITE, a protein domain database for functional characterization and annotation. *Nucleic Acids Res*. 2010; 38:D161–6. [PubMed: 19858104]

39. de Castro E, Sigrist CJ, Gattiker A, Bulliard V, Langendijk-Genevaux PS, Gasteiger E, et al. ScanProsite: detection of PROSITE signature matches and ProRule-associated functional and structural residues in proteins. *Nucleic Acids Res.* 2006; 34:W362–5. [PubMed: 16845026]
40. Gough J, Karplus K, Hughey R, Chothia C. Assignment of homology to genome sequences using a library of hidden Markov models that represent all proteins of known structure. *J Mol Biol.* 2001; 313:903–19. [PubMed: 11697912]
41. Schultz J, Milpetz F, Bork P, Ponting CP. SMART, a simple modular architecture research tool: identification of signaling domains. *Proceedings of the National Academy of Sciences of the United States of America.* 1998; 95:5857–64. [PubMed: 9600884]
42. Letunic I, Doerks T, Bork P. SMART 6: recent updates and new developments. *Nucleic Acids Res.* 2009; 37:D229–32. [PubMed: 18978020]
43. Zuckerkandl E, Pauling L. Molecules as documents of evolutionary history. *Journal of theoretical biology.* 1965; 8:357–66. [PubMed: 5876245]
44. Saitou N, Nei M. The neighbor-joining method: a new method for reconstructing phylogenetic trees. *Molecular biology and evolution.* 1987; 4:406–25. [PubMed: 3447015]
45. Tamura K, Peterson D, Peterson N, Stecher G, Nei M, Kumar S. MEGA5: molecular evolutionary genetics analysis using maximum likelihood, evolutionary distance, and maximum parsimony methods. *Molecular biology and evolution.* 2011; 28:2731–9. [PubMed: 21546353]
46. Cole C, Barber JD, Barton GJ. The Jpred 3 secondary structure prediction server. *Nucleic Acids Res.* 2008; 36:W197–201. [PubMed: 18463136]
47. Bryson K, McGuffin LJ, Marsden RL, Ward JJ, Sodhi JS, Jones DT. Protein structure prediction servers at University College London. *Nucleic Acids Res.* 2005; 33:W36–8. [PubMed: 15980489]
48. Jones DT. Protein secondary structure prediction based on position-specific scoring matrices. *J Mol Biol.* 1999; 292:195–202. [PubMed: 10493868]
49. Blom N, Gammeltoft S, Brunak S. Sequence and structure-based prediction of eukaryotic protein phosphorylation sites. *J Mol Biol.* 1999; 294:1351–62. [PubMed: 10600390]
50. Blom N, Sicheritz-Ponten T, Gupta R, Gammeltoft S, Brunak S. Prediction of post-translational glycosylation and phosphorylation of proteins from the amino acid sequence. *Proteomics.* 2004; 4:1633–49. [PubMed: 15174133]
51. Petersen TN, Brunak S, von Heijne G, Nielsen H. SignalP 4.0: discriminating signal peptides from transmembrane regions. *Nat Methods.* 2011; 8:785–6. [PubMed: 21959131]
52. Zuegge J, Ralph S, Schmuker M, McFadden GI, Schneider G. Deciphering apicoplast targeting signals—feature extraction from nuclear-encoded precursors of *Plasmodium falciparum* apicoplast proteins. *Gene.* 2001; 280:19–26. [PubMed: 11738814]
53. Waller RF, Keeling PJ, Donald RG, Striepen B, Handman E, Lang-Unnasch N, et al. Nuclear-encoded proteins target to the plastid in *Toxoplasma gondii* and *Plasmodium falciparum*. *Proceedings of the National Academy of Sciences of the United States of America.* 1998; 95:12352–7. [PubMed: 9770490]
54. Waller RF, Reed MB, Cowman AF, McFadden GI. Protein trafficking to the plastid of *Plasmodium falciparum* is via the secretory pathway. *Embo J.* 2000; 19:1794–802. [PubMed: 10775264]
55. Bologna G, Yvon C, Duvaud S, Veuthey AL. N-Terminal myristoylation predictions by ensembles of neural networks. *Proteomics.* 2004; 4:1626–32. [PubMed: 15174132]
56. Arnold K, Bordoli L, Kopp J, Schwede T. The SWISS-MODEL workspace: a web-based environment for protein structure homology modelling. *Bioinformatics.* 2006; 22:195–201. [PubMed: 16301204]
57. Kiefer F, Arnold K, Kunzli M, Bordoli L, Schwede T. The SWISS-MODEL Repository and associated resources. *Nucleic Acids Res.* 2009; 37:D387–92. [PubMed: 18931379]
58. Schwede T, Kopp J, Guex N, Peitsch MC. SWISS-MODEL: An automated protein homology-modeling server. *Nucleic Acids Res.* 2003; 31:3381–5. [PubMed: 12824332]
59. Guex N, Peitsch MC. SWISS-MODEL and the Swiss-PdbViewer: an environment for comparative protein modeling. *Electrophoresis.* 1997; 18:2714–23. [PubMed: 9504803]
60. Stewart AE, Dowd S, Keyse SM, McDonald NQ. Crystal structure of the MAPK phosphatase Pyst1 catalytic domain and implications for regulated activation. *America.* 1999; 6:174–82.

61. Bordoli L, Kiefer F, Arnold K, Benkert P, Battey J, Schwede T. Protein structure homology modeling using SWISS-MODEL workspace. *Nat Protoc.* 2009; 4:1–13. [PubMed: 19131951]
62. Laskowski RA, Rullmannn JA, MacArthur MW, Kaptein R, Thornton JM. AQUA and PROCHECK-NMR: programs for checking the quality of protein structures solved by NMR. *J Biomol NMR.* 1996; 8:477–86. [PubMed: 9008363]
63. Vriend G. WHAT IF: a molecular modeling and drug design program. *J Mol Graph.* 1990; 8:52–6. 29. [PubMed: 2268628]
64. Colovos C, Yeates TO. Verification of protein structures: patterns of nonbonded atomic interactions. *Protein science: a publication of the Protein Society.* 1993; 2:1511–9. [PubMed: 8401235]
65. Trivedi V, Nag S. In silico characterization of atypical kinase PFD0975w from *Plasmodium* kinome: a suitable target for drug discovery. *Chemical biology & drug design.* 2012; 79:600–9. [PubMed: 22233458]
66. Bowie JU, Luthy R, Eisenberg D. A method to identify protein sequences that fold into a known three-dimensional structure. *Science.* 1991; 253:164–70. [PubMed: 1853201]
67. Luthy R, Bowie JU, Eisenberg D. Assessment of protein models with three-dimensional profiles. *Nature.* 1992; 356:83–5. [PubMed: 1538787]
68. Laurie AT, Jackson RM. Q-SiteFinder: an energy-based method for the prediction of protein-ligand binding sites. *Bioinformatics.* 2005; 21:1908–16. [PubMed: 15701681]
69. Burgoyne NJ, Jackson RM. Predicting protein interaction sites: binding hot-spots in protein-protein and protein-ligand interfaces. *Bioinformatics.* 2006; 22:1335–42. [PubMed: 16522669]
70. Hendlich M, Rippmann F, Barnickel G. LIGSITE: automatic and efficient detection of potential small molecule-binding sites in proteins. *Journal of molecular graphics & modelling.* 1997; 15:359–63. 89. [PubMed: 9704298]
71. Liang J, Edelsbrunner H, Woodward C. Anatomy of protein pockets and cavities: measurement of binding site geometry and implications for ligand design. *Protein science: a publication of the Protein Society.* 1998; 7:1884–97. [PubMed: 9761470]
72. Liang J, Edelsbrunner H, Fu P, Sudhakar PV, Subramaniam S. Analytical shape computation of macromolecules: II. Inaccessible cavities in proteins. *Proteins.* 1998; 33:18–29. [PubMed: 9741841]
73. Kaminski GA, Friesner RA, Tirado-Rives J, Jorgensen WL. Evaluation and Reparametrization of the OPLS-AA Force Field for Proteins via Comparison with Accurate Quantum Chemical Calculations on Peptides. *Journal of Physical Chemistry.* 2001:6474–87.
74. Friesner RA, Banks JL, Murphy RB, Halgren TA, Klicic JJ, Mainz DT, et al. Glide: a new approach for rapid, accurate docking and scoring. 1. Method and assessment of docking accuracy. *Journal of medicinal chemistry.* 2004; 47:1739–49. [PubMed: 15027865]
75. Friesner RA, Murphy RB, Repasky MP, Frye LL, Greenwood JR, Halgren TA, et al. Extra precision glide: docking and scoring incorporating a model of hydrophobic enclosure for protein-ligand complexes. *Journal of medicinal chemistry.* 2006; 49:6177–96. [PubMed: 17034125]
76. MR4. *Methods in Malaria Research.* Paris, France: Malaria Research and Reference Reagent Resource Center; 2008.
77. Plouffe D, Brinker A, McNamara C, Henson K, Kato N, Kuhen K, et al. In silico activity profiling reveals the mechanism of action of antimalarials discovered in a high-throughput screen. *Proceedings of the National Academy of Sciences of the United States of America.* 2008; 105:9059–64. [PubMed: 18579783]
78. Lipinski C. Lead- and drug-like compounds: the rule-of-five revolution. *Drug discovery today.* 2004; 1:337–41. [PubMed: 24981612]
79. Ham S. Studies on Menadione as an Inhibitor of the cdc25 Phosphatase. *Bioorganic Chemistry.* 1997; 25:33–6.
80. Brohm D, Philippe N, Metzger S, Bhargava A, Müller O, Lieb F, et al. Solid-phase synthesis of dysidiolide-derived protein phosphatase inhibitors. *Journal of the American Chemical Society.* 2002; 124:13171–8. [PubMed: 12405845]
81. Dobson S, May T, Berriman M, Del Vecchio C, Fairlamb aH, Chakrabarti D, et al. Characterization of protein Ser/Thr phosphatases of the malaria parasite, *Plasmodium falciparum*:

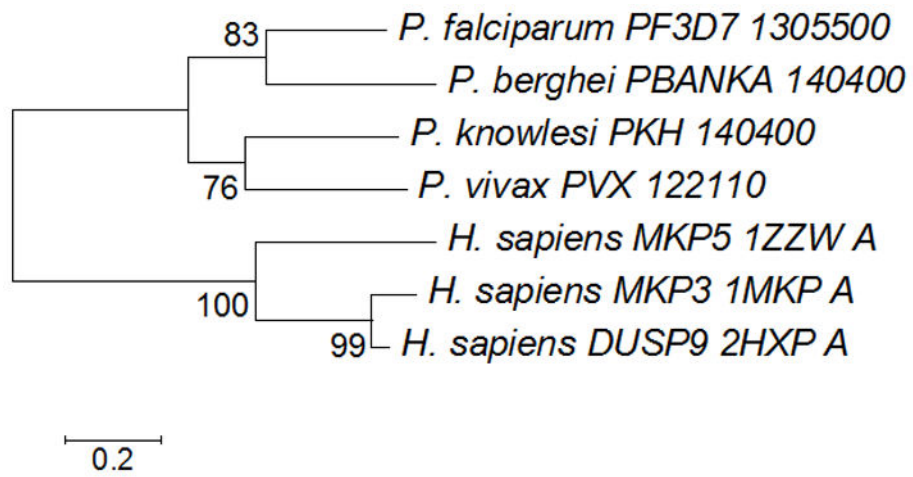
- inhibition of the parasitic calcineurin by cyclophilin-cyclosporin complex. *Molecular and biochemical parasitology*. 1999; 99:167–81. [PubMed: 10340482]
82. Contour-Galcera MO, Sidhu A, Prevost G, Bigg D, Ducommun B. What's new on CDC25 phosphatase inhibitors. *Pharmacology & therapeutics*. 2007; 115:1–12. [PubMed: 17531323]
83. Ludin P, Woodcroft B, Ralph S, Maser P. In silico prediction of antimalarial drug target candidates. *Int J Parasitol*. 2012; 2:191–9.
84. Delves M, Plouffe D, Scheurer C, Meister S, Wittlin S, Winzeler EA, et al. The activities of current antimalarial drugs on the life cycle stages of *Plasmodium*: a comparative study with human and rodent parasites. *PLoS Med*. 2012; 9:e1001169. [PubMed: 22363211]
85. Enayati A, Hemingway J. Malaria management: past, present, and future. *Annual review of entomology*. 2010; 55:569–91.
86. Gustin MC, Albertyn J, Alexander M, Davenport K. MAP kinase pathways in the yeast *Saccharomyces cerevisiae*. *Microbiol Mol Biol Rev*. 1998; 62:1264–300. [PubMed: 9841672]
87. Rangarajan R, Bei AK, Jethwaney D, Maldonado P, Dorin D, Sultan AA, et al. A Mitogen-activated Protein Kinase Regulates Male Gametogenesis and Transmission of the Malaria Parasite *Plasmodium berghei*. *EMBO reports*. 2005; 6:464–9. [PubMed: 15864297]
88. Dorin-Semlat D, Quashie N, Halbert J, Sicard A, Doerig C, Peat E, et al. Functional characterization of both MAP kinases of the human malaria parasite *Plasmodium falciparum* by reverse genetics. *Molecular microbiology*. 2007; 65:1170–80. [PubMed: 17651389]
89. Owens DM, Keyse SM. Differential regulation of MAP kinase signalling by dual-specificity protein phosphatases. *Oncogene*. 2007; 26:3203–13. [PubMed: 17496916]
90. Low H, Chua CS, Sim T-S. Regulation of *Plasmodium falciparum* Pfnek3 relies on phosphorylation at its activation loop and at threonine 82. *Cellular and molecular life sciences: CMLS*. 2009; 66:3081–90. [PubMed: 19644735]
91. Surachetpong W, Singh N, Cheung KW, Luckhart S. MAPK ERK signaling regulates the TGF-beta1-dependent mosquito response to *Plasmodium falciparum*. *PLoS pathogens*. 2009; 5:e1000366. [PubMed: 19343212]
92. Gardner MJ, Hall N, Fung E, White O, Berriman M, Hyman RW, et al. Genome sequence of the human malaria parasite *Plasmodium falciparum*. *Nature*. 2002; 419:498–511. [PubMed: 12368864]
93. Gagaring, K.; Borboa, R.; Francek, C.; Chen, Z.; Buenviaje, J.; Plouffe, D., et al. Novartis. Novartis-GNF Malaria Box Dataset. Genomics Institute of the Novartis Research Foundation (GNF); 2010. Novartis-GNF Malaria Box Dataset.
94. Guiguemde WA, Shelat AA, Bouck D, Duffy S, Crowther GJ, Davis PH, et al. Chemical genetics of *Plasmodium falciparum*. *Nature*. 2010; 465:311–5. [PubMed: 20485428]
95. Lye YM, Chan M, Sim TS. Pfnek3: an atypical activator of a MAP kinase in *Plasmodium falciparum*. *FEBS Lett*. 2006; 580:6083–92. [PubMed: 17064692]
96. McGovern SL, Shoichet BK. Information decay in molecular docking screens against holo, apo, and modeled conformations of enzymes. *Journal of medicinal chemistry*. 2003; 46:2895–907. [PubMed: 12825931]

```

PF3D7_1305500: ALCTNQVQLNNTSF-----IKQNKQLICYINSTHNKKQNMNNQNNLIICNHGMKNPTS-EKTNSSLIICMCIYIMYIKKYNPNLIIAYMLKIYNNW
PKH_140400:   SGNADRQRIVKGTHMEKSSATADRRHSQKKAMLN---ISNKQNMQNGN-ILIMCNHGMKNRRR-EKINSSLVIAMCYLMYTRRYDPNLIASVLRINNNF
PVX_122110:   KGVKETQMEKPN-----AGAGGKPSKKMAWLS---NPYEGSLQNGN-VIIVCNEGMYQTK-GKNNSSLIIMCYLMYTKKCGPNLTIAYVLRINNNI
PBANKA_140400: DVKKENSQNEINE-----SGKNILENNAIIN---NNKYQPNNLKKNLIICNDGIKDESNKQKINSSLIISMCIYIYSKYINLNLAIAYMIKICNNL
MKP3_1MKP_A:   KYKQIPSNSNSQN-----LSQFPEASFID---EARCKNGC---VLVHCLACI-----SQSVTVTVAVYLMQKLNLSMNDAYDIVKMKSNI
DUSP9_2HXP_A: HYKQIPSNSNSQN-----LSRFPEAIEFIED---EALSONCG---VLVHCLAGV-----SQSVTVTVAVYLMQKLNLSMNDAYDIVKMKSNI
MKP5_1ZZW_A:   NYKRLPATNSNKQN-----LRQYFEEAFEFEIE---EA--HQCGKG--LLIHCQAGV-----SQSVTVTVAVYLMQKLNLSMNDAYDIVKMKSNI
    
```

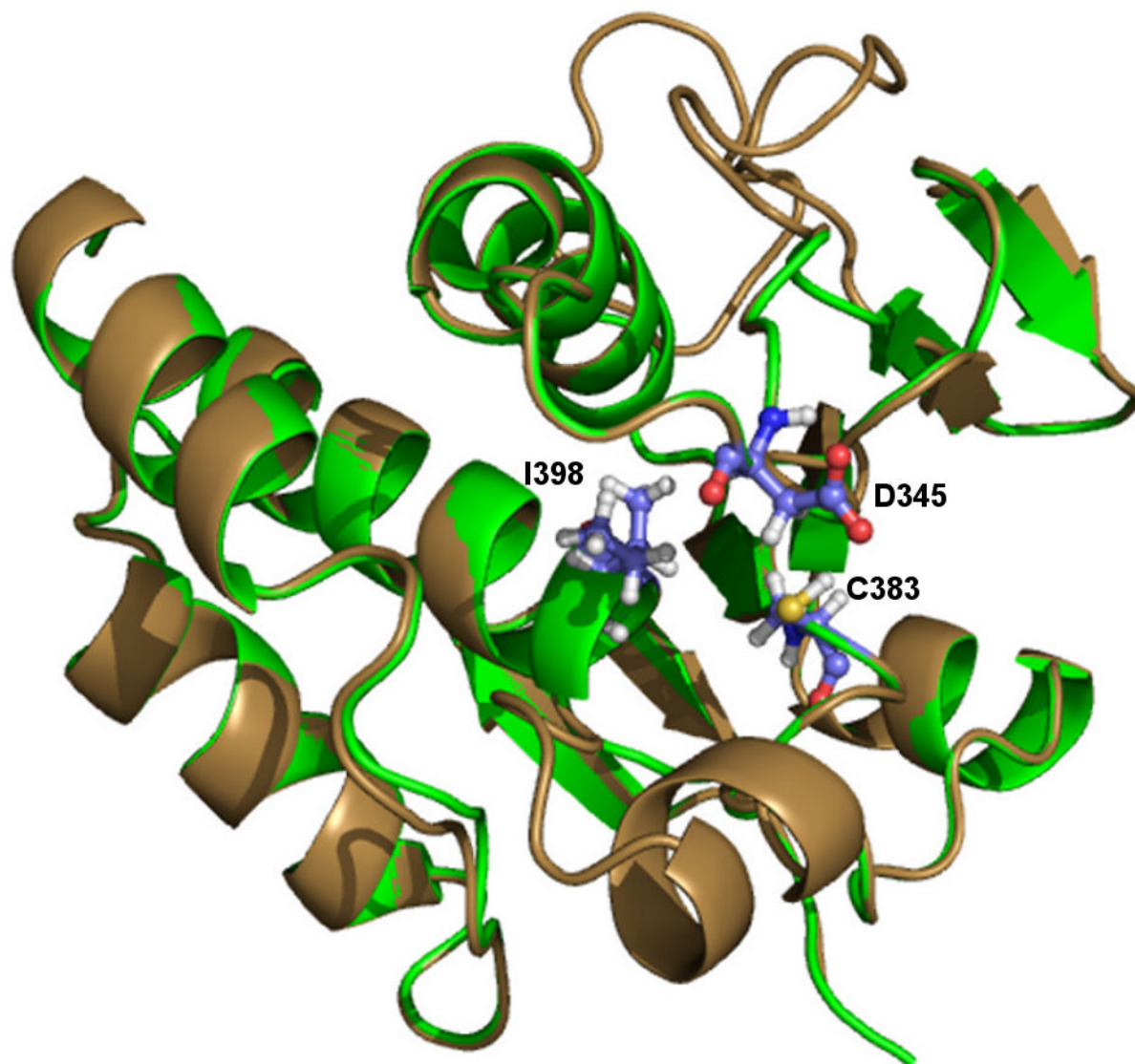
**Figure 1.**

Multiple sequence alignment of protozoan orthologs of PF2D7\_1305500 with potential templates. Potential templates were identified from BLAST searches in Swiss Model. The obtained sequences were aligned using CLUSTALW. The conserved binding pocket residues are highlighted in black (■ ■ ■), whereas the main deviation in the binding pocket residues is the presence of an isoleucine in the *Plasmodium* sequences, which aligns with arginine present in the template sequences is highlighted in grey (■). Additionally there are additional residues in the region of the binding pocket following the cysteine. These two alterations are conserved in the *Plasmodium* sequences. Sequence orthologs in the alignment are from *P. falciparum* (PF3D7\_1305500), *P. knowlesi* (PKH\_140400), *P. vivax* (PVX\_122110), *P. berghei* (PBANKA\_140400) and *Homo sapien* (MKP3\_1MKP\_A, DUSP9\_2HXP\_A, MKP5\_1ZZW\_A).

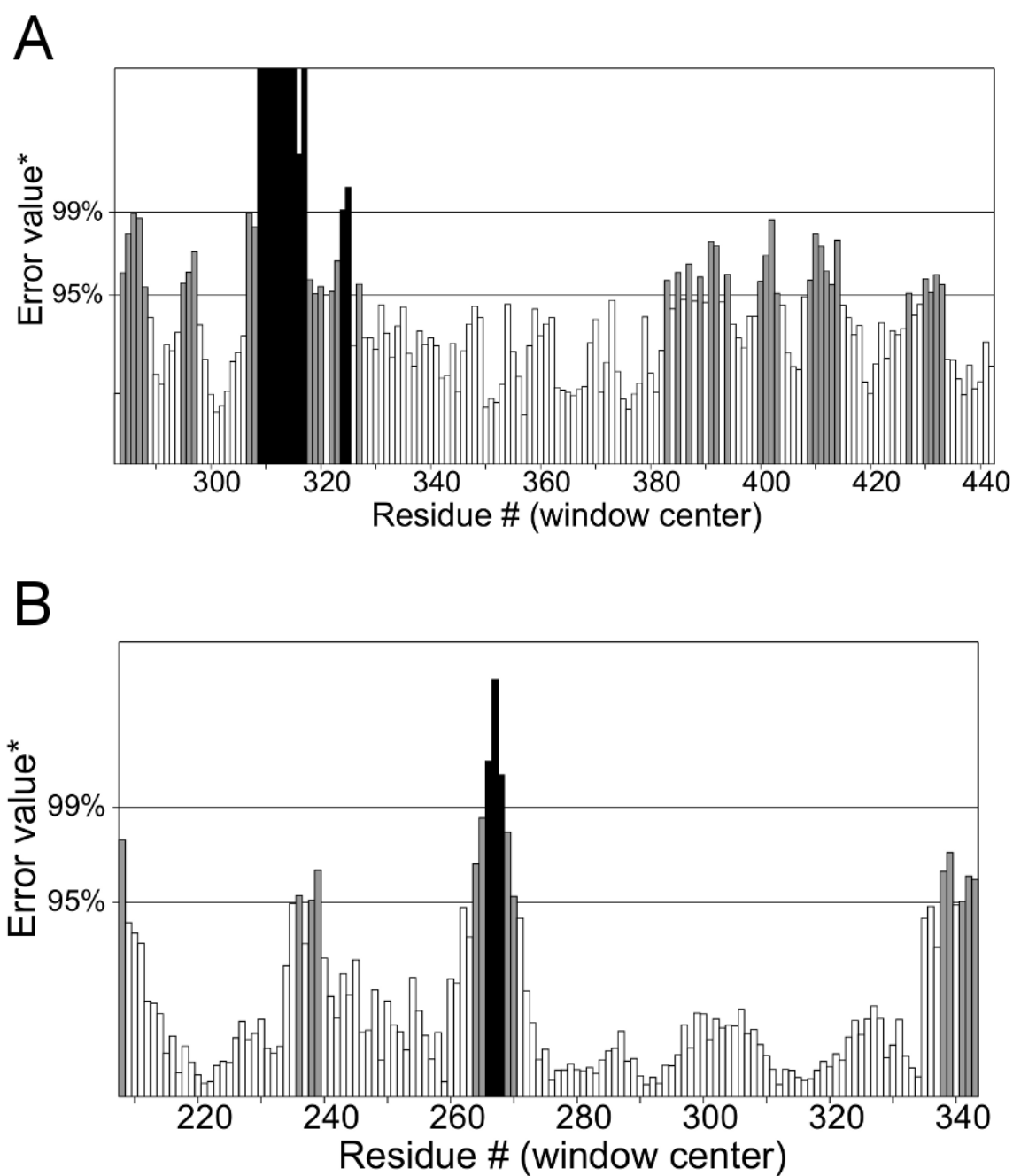


**Figure 2.** Phylogenetic analysis of PF3D7\_1305500. The Neighbor-Joining method was used to construct the evolutionary history of the atypical phosphatase using the bootstrap test with 1000 replicates. The evolutionary distances were computed using the Poisson correction method.

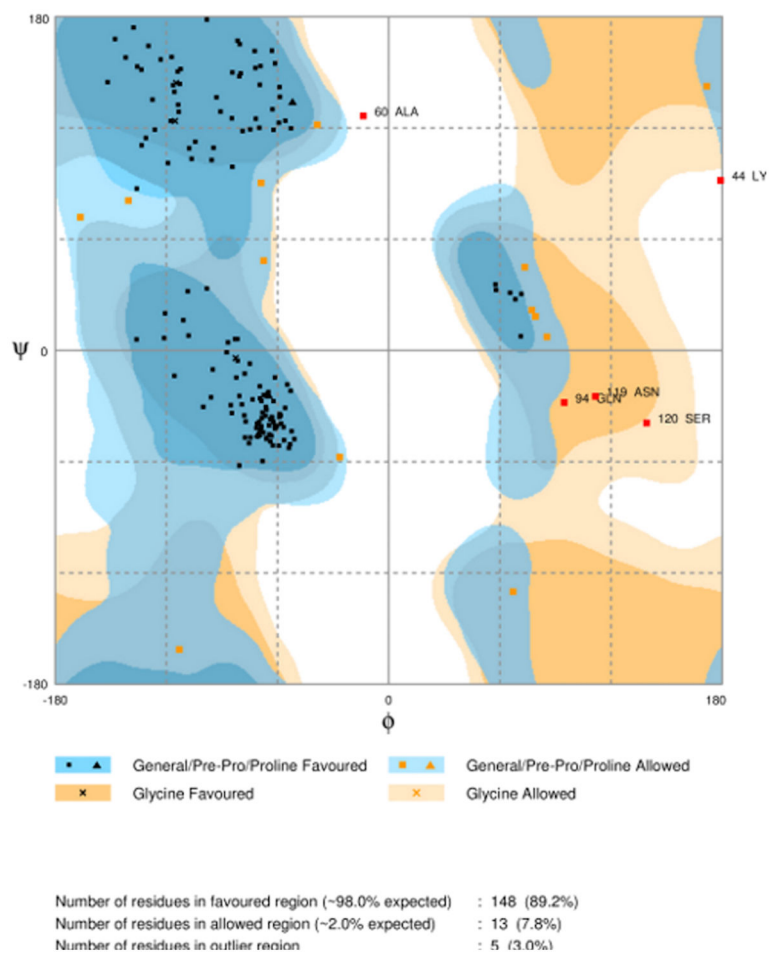




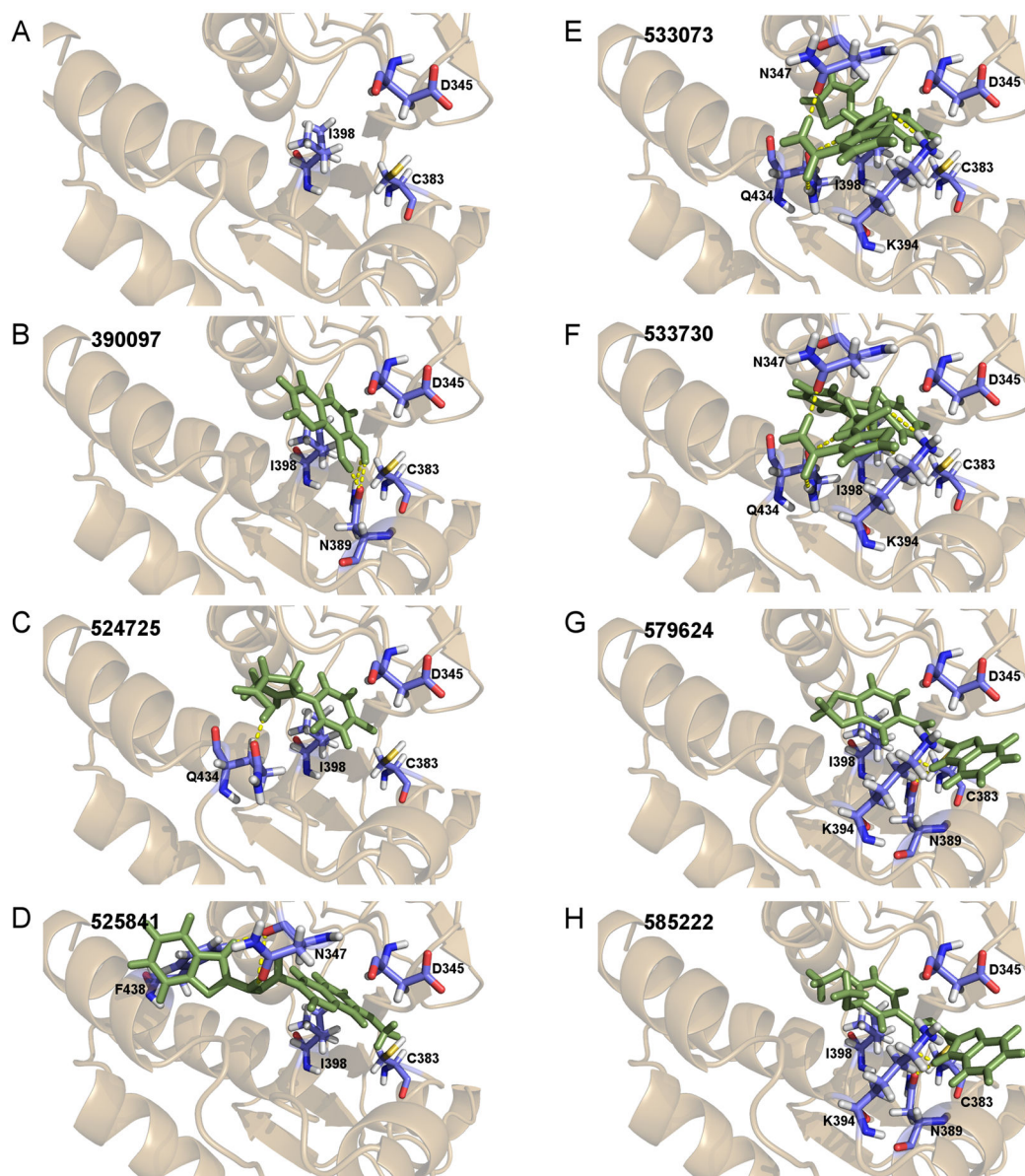
**Figure 3.** Homology model of PF3D7\_1305500. The structure of PF3D7\_1305500 (brown) was developed using the crystal structure of MKP3 as a template (PDB 1MKP). Alignment of the model with MKP3 (green) revealed that the final structure showed the catalytic residues aligned to the proposed positions in the active site. The presence of the signature motif insertion does not affect the shape of the active site and forms an alpha-helix adjacent to the binding pocket without obstructing the site.



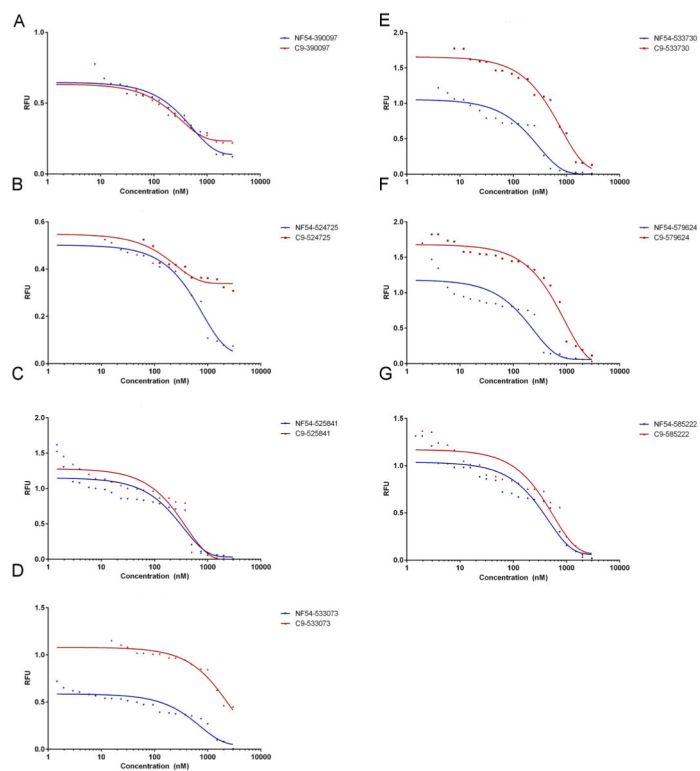
**Figure 4.** Overall quality assessment of the model evaluated using ERRAT. The figures compare the template crystal structure and homology model for (A) PF3D7\_1305500 and (B) MKP3.



**Figure 5.** Ramachandran plot. The quality of the homology model was validated and found to have 89.2% of the residues in favorable positions.



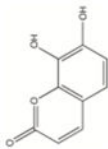
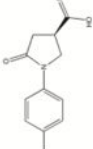
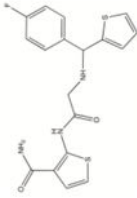
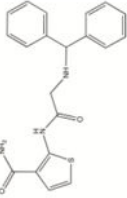
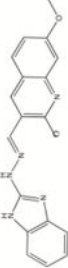

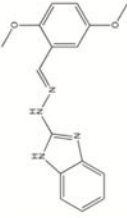
**Figure 6.** DUSP domain virtual screen. The homology model structure of the binding site of the PF3D7\_1305500 DUSP domain was used for an *in silico* virtual screen of compound structures in ChEMBL database. (A) The binding pocket is surrounded by three conserved residues (D345, C383, I398) thought to be involved in substrate binding. Additional residues adjacent to the binding pocket with predicted polar interaction of the ligands were also included. (B–H) This pocket was targeted for virtual screening and 7 of the compounds with greatest affinity to this site were identified.



**Figure 7.** SYBR green I assay of selected compounds. Mean  $EC_{50}$  values were calculated and plotted in GraphPad Prism 6. Three compounds 533073, 533730 and 579624 shows significantly lower activity against C9 parasites.

Table 1

Selected ChEMBL-NTD compounds used for *in vitro* screening.

Structure	ChEMBL ID	Name	MW	LogP	HBA	HBD	Score
	390097	7,8-Dihydroxy-2H-chromen-2-one	178.1	1.42	4	2	-8.35
	524725	1-(4-Chlorophenyl)-5-oxo-3-pyrrolidinecarboxylic acid	239.6	1.40	3	1	-8.41
	533073	2-((N-((4-Fluorophenyl)(2-thienyl)methyl)glycyl)amino)-3-thiophenecarboxamide	389.5	2.46	3	3	-8.29
	533730	2-((N-(Diphenylmethyl)glycyl)amino)-3-thiophenecarboxamide	365.5	2.40	3	3	-8.42
	525841	3-((E)-(1H-Benzimidazol-2-ylhydrazono)methyl)-2-chloro-7-methoxyquinoline	351.8	3.91	5	2	-8.36
	579624	2-((2E)-2-(1,3-Benzodioxol-5-ylmethylene)hydrazino)-1H-benzimidazole	280.3	3.27	6	2	-7.23
	585222	2-((2E)-2-(3,4-Dimethoxybenzylidene)hydrazino)-1H-benzimidazole	298.3	3.47	6	2	-7.44



**Table 2**

Comparison of NF54 and C9 susceptibility to the selected compounds. EC<sub>50</sub> values obtained from treating the wild type (NF54) and PF3D7\_1305500 (C9) parasites were compared using the Mann-Whitney test ( $\alpha=0.05$ ). Compounds 5333073, 533730 and 579624 show NF54 to have significantly greater susceptibility ( $p<0.05$ ). This suggests that C9 parasites may have a slight advantage when not expressing the predicted target.

Compound ID	EC <sub>50</sub> NF54 (nM)	EC <sub>50</sub> C9 (nM)	<i>p</i>
390097	340.2±53.6	248.9±33.7	0.1124
524725	503.1±36.5	248.4±62	0.0240
533073	471.9±37.4	1227.3±86.3	0.0013
533730	196.3±113.8	510.9±51.6	0.0073
525841	186.1±33.8	224.7±48.1	0.5467
579624	136±33.1	584±39.86	0.0010
585222	378.8±97.7	339.3±28	0.7070